

Orbital Variability in the Eclipsing Pulsar Binary PSR B1957+20

Z. Arzoumanian,¹ A. S. Fruchter,² AND J. H. Taylor³

Abstract

We have conducted timing observations of the eclipsing millisecond binary pulsar PSR B1957+20, extending the span of data on this pulsar to more than five years. During this time the orbital period of the system has varied by roughly $\Delta P_b/P_b = 1.6 \times 10^{-7}$, changing quadratically with time and displaying an orbital period second derivative $\ddot{P}_b = (1.43 \pm 0.08) \times 10^{-18} \text{ s}^{-1}$. The previous measurement of a large negative orbital period derivative reflected only the short-term behavior of the system during the early observations; the orbital period derivative is now positive and increasing rapidly. If, as we suspect, the PSR B1957+20 system is undergoing quasi-cyclic orbital period variations similar to those found in other close binaries such as Algol and RS CVn, then the $0.025 M_\odot$ companion to PSR B1957+20 is most likely non-degenerate, convective, and magnetically active.

Subject headings: pulsars — binaries: evolution — stars: eclipsing binaries — stars: individual (PSR B1957+20)

1 Introduction

The evolutionary links between solitary millisecond pulsars and their presumed binary progenitor systems may involve a number of exotic astrophysical phenomena. In their late stages of evolution, neutron stars in low-mass X-ray and pulsar binaries may evaporate their companions through the strength of their radiation, turning themselves into solitary “recycled” pulsars (Alpar *et al.* 1982; Ruderman, Shaham & Tavani 1989; Bhattacharya & van den Heuvel 1991). In some cases, material from the companion may even reform to create planets (Banit & Shaham 1992; Tavani & Brookshaw 1992; Stevens, Rees & Podsiadlowski 1992). The discovery of PSR B1957+20 (Fruchter, Stinebring & Taylor 1988), a 1.6 ms pulsar in orbit with a $\sim 0.025 M_\odot$ companion, has provided the strongest evidence that this scenario actually occurs in nature, and that interacting binary systems are indeed responsible for the creation of the fastest pulsars.

In spite of the small size of its companion, the pulsar’s radio signal is eclipsed over approximately ten percent of the 9.2 hour orbit. Excess delays of the pulses are observed for many minutes after eclipse egress but only briefly before ingress, revealing the existence

¹Joseph Henry Laboratories and Department of Physics, Princeton University, Princeton, NJ 08544.
E-mail: Internet, zaven@pulsar.princeton.edu

²Astronomy Department and Radio Astronomy Laboratory, University of California, Berkeley, CA 94720.
E-mail: Internet, asf@orestes.berkeley.edu
Hubble Fellow

³Joseph Henry Laboratories and Department of Physics, Princeton University.
E-mail: Internet, joe@pulsar.princeton.edu

of an ionized wind from the companion which is continuously infused with new matter (Fruchter *et al.* 1990, hereafter F90) and is responsible for the radio eclipse. Optical observations of the companion provide estimates of its temperature, radius and thermal timescale (Fruchter & Goss 1992 and references therein), and show a strong modulation with orbital phase of its optical luminosity consistent with irradiation from the pulsar. Radio observations show the electron column density in the evaporated wind to be small (F90; Ryba & Taylor 1991, hereafter RT91), a result supported by observed transparency of the wind to unpulsed emission at $\lambda = 20$ cm (Fruchter & Goss 1992). However, RT91 also reported a large (negative) orbital period derivative over the ~ 2.5 years spanned by their observations, seemingly implying an unexpectedly short timescale of 30 Myr for orbital decay. This conclusion was difficult to reconcile with the low rate of mass loss suggested by the density of the companion’s wind.

We have conducted further timing observations of PSR B1957+20 beginning in November 1992 and spanning 9 months. Together with the earlier timing measurements described in F90 and RT91, our data reveal orbital evolution previously unobserved in binary systems containing a pulsar: the orbital period derivative (\dot{P}_b) of the PSR B1957+20 system has changed sign and has been increasing steadily.

2 Observations and Analysis

Our observations of PSR B1957+20 were carried out at the Arecibo Observatory using the Princeton Mark III system (Stinebring *et al.* 1992), the same data acquisition system used by F90 and RT91. The pulsar signal was coherently de-dispersed, detected, and synchronously averaged during integrations lasting approximately two minutes. Accurate integration start times were provided by a local rubidium clock, traceable via GPS to UTC. All of our observations were made at frequencies in the range 426–434 MHz; two passbands of width 0.41 MHz were coherently dedispersed, their center frequencies chosen to track scintillation-induced maxima in the signal strength. Dual circularly polarized signals were then summed to form a total-intensity profile of pulse strength versus rotational phase. Pulse times-of-arrival (TOAs) were computed by fitting observed profiles to a low-noise template and adding the resulting phase offset to a time near the midpoint of the integration, derived by adding an integer number of pulse periods to the start time. TOAs collected during 15-minute intervals were then averaged. The entire data set, including the measurements of F90 and RT91, consists of 253 averaged TOAs obtained between 24 March 1988 and 12 September 1991, and 111 between 19 November 1992 and 11 June 1993. Heavy scheduling demands on the Arecibo telescope and a timing campaign of several new millisecond pulsars discovered at similar right ascensions are responsible for the one year gap in the data. A concentrated observing session designed to yield well-sampled, redundant coverage of the orbit was carried out during 14–20 April 1993.

We have used a modified version of the TEMPO software package (Taylor & Weisberg 1989) to reduce the topocentric TOAs to the solar system barycenter established by the DE200 solar system ephemeris (Standish 1982), and perform a multi-parameter fit to the spin, astrometric and orbital parameters of the pulsar by minimizing the sum of squares of

the differences between predicted and observed TOAs. Parameters of the model include the pulsar’s rotational phase, frequency and as many as six frequency derivatives (see below), dispersion measure, position and proper motion, the projected semi-major axis of its orbit, its orbital period and phase, two derivatives of the orbital period, and optionally, orbital eccentricity, angle of periastron and semi-major axis rate of change. In all fits, pulse arrival times between orbital phases 0.19 and 0.39 (which we refer to as the “timing eclipse”) were given zero weight; within this region, the pulses are either eclipsed or unpredictably delayed as they travel through the companion’s wind (see F90, RT91).

The residuals from our multi-parameter fits display long-term unmodeled fluctuations which appear as correlated noise in the pulse arrival times (see Figure 1). The magnitude of these residuals is consistent with changes in the dispersion measure of the pulsar expected from its motion through the interstellar medium (see, e.g., Backer *et al.* 1993), and we believe this to be the most likely explanation of the noise. These residuals could also be due, however, to changes in ablated material surrounding the pulsar, or perhaps rotational irregularities in the neutron star itself. (The existence of “timing noise” in millisecond pulsars is discussed in Kaspi, Taylor & Ryba 1994.) Since least-squares parameter estimation is unreliable when naïvely applied in the presence of such noise, in addition to fitting the average deterministic spin-down behavior of the pulsar, higher-order rotational derivatives $d^2\nu/dt^2$, $d^3\nu/dt^3$, ..., where $\nu = 1/P$, were introduced as free parameters in order to model and absorb the observed drifts in pulse phase. The astrometric and orbital parameters obtained from such a fit were adopted as the best unbiased values, and these appear in Table 1. Since systematic parameter biases introduced by timing noise are much larger than the formal uncertainties in these fits, we carried out a number of fits in which the modeled timing noise was replaced by simulated noise; we used the resulting distributions of parameter values to obtain 1σ estimates of the uncertainty associated with each parameter. The simulated noise was constructed to be similar in spectral content to the modeled noise (represented by the high-order spin frequency derivatives) but with arbitrary phases. Finally, to obtain the deterministic spin parameters of the pulsar (pulse phase, frequency, and frequency first derivative) and to best display the timing noise, these parameters were fit with the celestial and orbital parameters held fixed at their adopted values. The resulting residuals are plotted versus date and orbital phase in Figure 1. Note that much of the power in the “reddest” components of the timing noise spectrum is absorbed in our fit for the average spin period and period derivative. These quantities can therefore be expected to differ, in fits which span different epochs, by more than their measurement uncertainties. We have not attempted to correct for any parameter bias in the global spin period and its derivative, and so quote statistical uncertainties only for these quantities. Because the orbital period is some three orders of magnitude smaller than the timescale of the timing noise, we believe that the fitted orbital parameters are not significantly contaminated by its effects.

The orbital eccentricity was held fixed at zero in all of our preferred timing solutions, and T_0 in Table 1 is a time near the center of the data set at which the pulsar crossed the ascending node, defined as the zero of orbital phase. A formal solution for the orbital eccentricity e and angle of periastron ω is in fact possible, but we prefer to quote the results

of such a fit as an upper limit to the eccentricity, since irregular sampling in orbital phase and an angle of periastron near eclipse egress lend little credence to the formal solution. In most instances and especially in the case of the pulsar’s astrometric parameters, the best-fit values presented in Table 1 improve significantly upon previous measurements. We see no substantial change in either the duration of eclipse or the magnitude of excess propagation delays in comparisons of our recent observations with the results of RT91, although these phenomena remain highly variable from one observation to the next. Further monitoring of PSR B1957+20 will add to the handful of eclipse events in our data set and may eventually constrain any changes to the eclipsing medium.

3 Results

As a check of the orbital behavior implied by our global fit, we divided our data into five non-overlapping subsets, each containing about one year of pulse arrival times. These were individually fit for P , \dot{P} , one or two additional rotational derivatives where necessary, and two orbital parameters, T_0 and P_b , at an epoch near the center of each subset while the pulsar’s position on the sky, determined from the proper motion, was held fixed. The resulting fractional orbital period changes are plotted in Figure 2a. A varying gravitational acceleration due to a second companion in a distant orbit or large fluctuations in dispersion measure could, in principle, produce changes in the apparent orbital period similar to those seen here. They would, however, also affect our measurement of the pulsar spin period, so that $\Delta P_b/P_b = \Delta P/P$. As Figure 2b shows, the spin period displays no such variation, at a level nearly five orders of magnitude less than that required. Apparent variations in orbital period due to such dynamical effects can therefore be ruled out. While both the transverse Doppler shift due to the pulsar’s proper motion and differential Galactic acceleration can introduce a spurious, essentially constant \dot{P}_b (Damour & Taylor 1991), we note that for PSR B1957+20 they together contribute to the observed orbital period derivative at a level comparable to the uncertainty in our measurement of \dot{P}_b .

Figure 3 displays the orbital phase shifts detected in the PSR B1957+20 system over more than 5 years. The points plotted in this “observed minus computed” diagram are deviations from the orbital ephemeris⁴

$$\phi_c = \frac{86400}{33001.9162448} [t(\text{MJD}) - T_0], \quad (1)$$

derived from our pulse arrival-time measurements. To obtain these differences, estimated TOAs were computed using only the best-fit astrometric and spin parameters (including additional frequency derivatives) and subtracted from the observed values. Non-zero residuals were thus assumed to be entirely due to orbital phase deviations from the pre-fit model. Residuals obtained during timing eclipse and within 0.06 of orbital phase 0.75 (inferior conjunction) were omitted since small random fluctuations at these phases result in

⁴The values of P_b and its derivatives compiled in Table 1 reflect a Taylor expansion of the orbital period about the center of the data span; by contrast, the value $P_b = 33001.9162448$ s in Equation (1) is roughly the *average* orbital period over the same span. The constant 86400 is the number of seconds in one day.

large apparent orbital phase shifts. The phase shifts derived from single integrations were then combined, with relative weights proportional to the cosine of the orbital phase, to form daily averages. The results of this process are plotted in Figure 3; error bars represent the RMS deviation from the mean of each daily average. The dominant cubic trend corresponds to the value of \ddot{P}_b derived from the global fit. Note that a decreasing slope (for example, from positive to negative after 1990) in the phase shifts of Figure 3 indicates a decrease in orbital frequency, or an increase in orbital period. This convention differs in sign from O–C diagrams derived from eclipse timings: we measure the difference in orbital phase at a given instant in time, while eclipse timing yields a difference in the time of passage through a specified orbital phase.

4 Discussion

Although our observations reveal that the orbital period derivative discovered by RT91 is not constant and thus provides little direct information on the ultimate fate of the companion of PSR B1957+20, we cannot entirely rule out the most popular explanation of that first measurement, that the orbital period changes are caused by substantial mass loss (Banit & Shaham 1992; Eichler 1992; Brookshaw & Tavani 1993; McCormick *et al.* 1994). Nonetheless, we find this proposition unlikely for a number of reasons. In order to transport sufficient angular momentum to produce the observed orbital period variations, the wind density must be several orders of magnitude higher than indicated by the electron density along the line of sight. Therefore, the bulk of the escaping material must either be hidden by the orbit’s inclination or be overwhelmingly neutral; the latter explanation seems particularly unlikely given the large systemic escape velocity and the intensity of the pulsar radiation. Furthermore, to match our present results the angular momentum carried by the ablated matter must have varied smoothly over the past five years while doubling in magnitude and changing sign.

We believe a more natural explanation is that PSR B1957+20 undergoes small quasi-periodic oscillations in orbital period. Orbital variations comparable in magnitude to those witnessed here are fairly common in short-period binaries containing a low-mass main-sequence star and have been well-studied in Algol and RS CVn systems (Söderhjelm 1980; Hall 1989; Warner 1988). In such binaries, rotation of the main-sequence star is likely to be tidally locked to the orbital period; as a result, the ratio of rotational timescale to convective timescale, the star’s “Rossby number,” is less than one. These stars are generally magnetically active and display substantial chromospheric activity, radio and x-ray flares and stellar winds 10^2 – 10^4 times stronger than slowly rotating stars of similar spectral class (Pasquini & Lindgren 1993; Simon 1990). The rapid rotation appears to maintain a magnetic dynamo which not only creates an energetic stellar atmosphere, but also distorts the star sufficiently to alter its gravitational quadrupole moment and, in turn, the orbital period (Applegate 1992).

If the companion to PSR B1957+20 is bloated and at least partially non-degenerate, as optical observations appear to imply (Aldcroft, Romani & Cordes 1992; Fruchter & Goss 1992), then the stellar atmosphere should be convective and have an overturn timescale far

in excess of the 9.2 hour binary period. The Rossby number of the companion would then be less than one and, like the binaries discussed above, the system might be expected to display orbital period variations and the companion a strong stellar wind, even in the absence of a pulsar primary. Although the companion’s external magnetic field is already constrained by Faraday delay measurements (less than a few gauss parallel to the line of sight at the edges of the eclipse region), a much stronger, toroidal, subsurface field could remain undetected by these observations. If this hypothesis is true, the truly peculiar aspect of the system is not the activity of the companion, but rather its non-degeneracy, for this star is far too light to be burning hydrogen. Either the present irradiation by the pulsar must be responsible for the swollen state of this object, perhaps through a mechanism similar to that proposed by Podsiadlowski (1991) for low-mass X-ray binaries, or evaporation of most of the companion’s mass must have been sufficiently recent that it has not yet had time to shrink to degeneracy.

We suspect that rotationally-induced magnetic activity not only explains much of the behavior of the PSR B1957+20 system, but may also be important in understanding observations of two other eclipsing pulsars in short-period binaries, PSRs B1744–24A (Lyne *et al.* 1990) and B1718–19 (Lyne *et al.* 1993). The companions of these pulsars are most likely low-mass main-sequence dwarfs, and in the case of PSR B1744–24A, the companion should nearly fill its Roche lobe. Both of these objects display evidence of excess material surrounding the entire binary, PSR B1744–24A through prolonged “anomalous” eclipses and pulse arrival delays (Lyne *et al.* 1990; Nice *et al.* 1990) and PSR B1718–19 through an inverted radio spectrum below 600 MHz. In each case, however, the energy density of the pulsar radiation impinging on the companion is far less than that to which the companion of PSR B1957+20 is exposed. (The observed spin-down rate of PSR B1744–24 is certainly contaminated by the system’s acceleration in the gravitational potential of its cluster, but the pulsar flux at the companion can be estimated by assuming an intrinsic period derivative similar to that of other millisecond pulsars, Nice & Thorsett 1992.) While pulsar irradiation would seem incapable of expelling the observed material from the companion surfaces, a rotationally powered wind, such as those found in RS CVn systems, could be sufficiently strong to produce the eclipses (a point that has been made independently by Wijers & Paczyński 1993 for PSR B1718–19) and could explain the seemingly “episodic” nature of the anomalous eclipses in PSR B1744–24A (Lyne *et al.* 1990; Nice & Thorsett 1992). One might expect to see orbital period variations in these other two eclipsing systems, but the low flux densities and long spin periods of these pulsars may make the required timing accuracy difficult to obtain.

M. F. Ryba and D. R. Stinebring built observing hardware and obtained some of the data that made this project possible. We are in their debt. We are also grateful to F. Camilo and A. Vázquez for observing assistance, and to D. J. Nice, B. Paczyński, and C. Thompson for helpful discussions. The Arecibo Observatory is part of the National Astronomy and Ionosphere Center, operated by Cornell University under cooperative agreement with the National Science Foundation. ASF was supported by a Hubble Fellowship awarded by NASA through the Space Telescope Science Institute.

Table 1: Astrometric, Spin, and Orbital Parameters of PSR B1957+20.

Right ascension, α (J2000) ^a	19 ^h 59 ^m 36 ^s .76988(5)
Declination, δ (J2000)	20° 48′ 15″.1222(6)
μ_α (mas yr ⁻¹)	-16.0 ± 0.5
μ_δ (mas yr ⁻¹)	-25.8 ± 0.6
Period, P (ms)	1.60740168480632(3)
Period derivative, \dot{P} (10 ⁻²⁰)	1.68515(9)
\ddot{P} (10 ⁻³¹ s ⁻¹)	1.4 ± 0.4
Epoch (MJD)	48196.0
Dispersion measure, DM (cm ⁻³ pc) ...	29.1168(7)
Projected semi-major axis, x (lt-s) ...	0.0892253(6)
Eccentricity, e	< 4 × 10 ⁻⁵
Epoch of ascending node, T_0 (MJD) ..	48196.0635242(6)
Orbital period, P_b (s)	33001.91484(8)
\dot{P}_b (10 ⁻¹¹)	1.47±0.08
\ddot{P}_b (10 ⁻¹⁸ s ⁻¹)	1.43±0.08
$ \ddot{\ddot{P}}_b $ (10 ⁻²⁶ s ⁻²)	< 3
$ \dot{x} $ (10 ⁻¹⁴)	< 3

^aCoordinates are given in the J2000 reference frame of the DE200 solar system ephemeris. Figures in parentheses are uncertainties in the last digits quoted.

References

- Aldcroft, T. L., Romani, R. W. & Cordes J. M. 1992, ApJ, 400, 638
- Alpar, M. A., Cheng, A. F., Ruderman, M. A. & Shaham J. 1982, Nature, 300, 728
- Applegate J. H. 1992, ApJ, 385, 621
- Backer, D. C., Hama, S., Van Hook, S. & Foster R. S. 1993, ApJ, 404, 636
- Banit, M. & Shaham J. 1992, ApJ, 388, L19
- Bhattacharya, D. & van den Heuvel, E. P. J. 1991, Phys.Rep., 203, 1
- Brookshaw, L. & Tavani M. 1993, ApJ, 410, 719
- Damour, T. & Taylor J. H. 1991, ApJ, 366, 501
- Eichler D. 1992, MNRAS, 254, 11P
- Fruchter, A. S., Berman, G., Bower, G., Convery, M., Goss, W. M., Hankins, T. H., Klein,

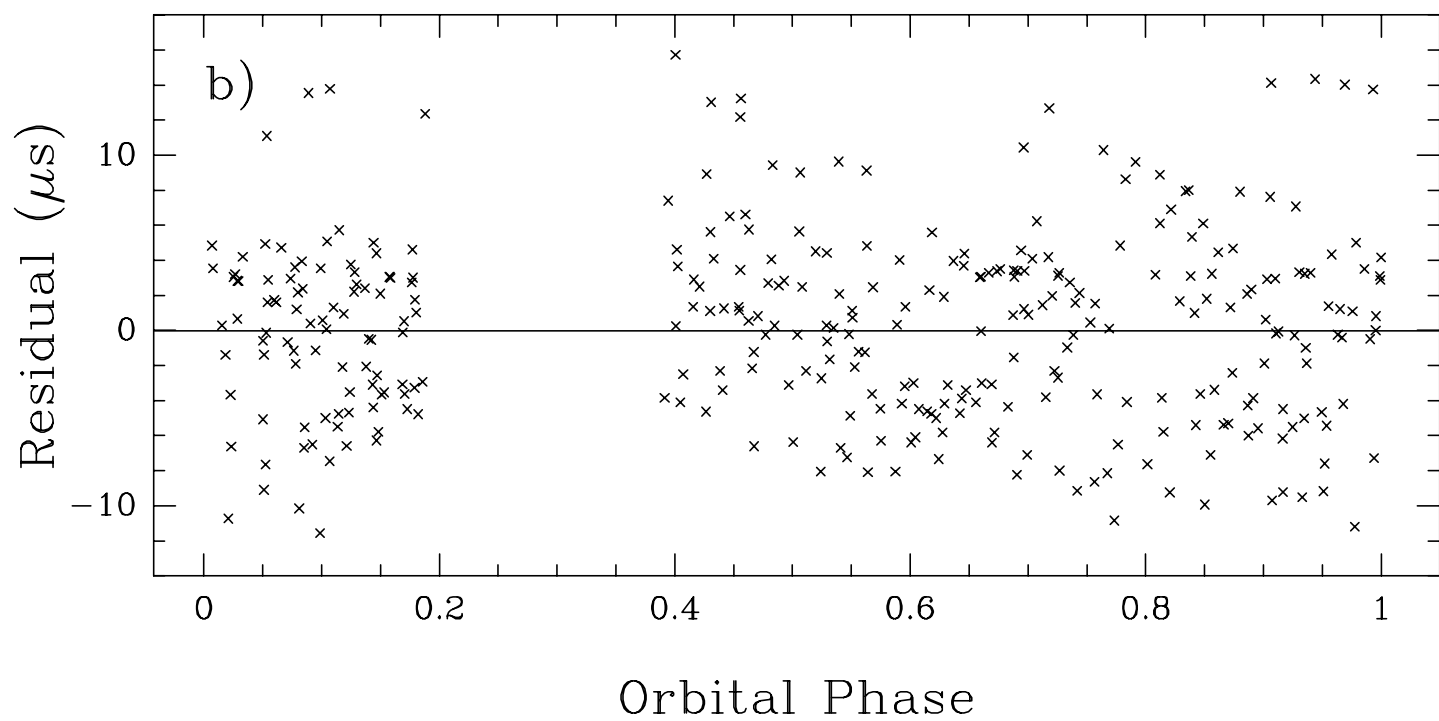
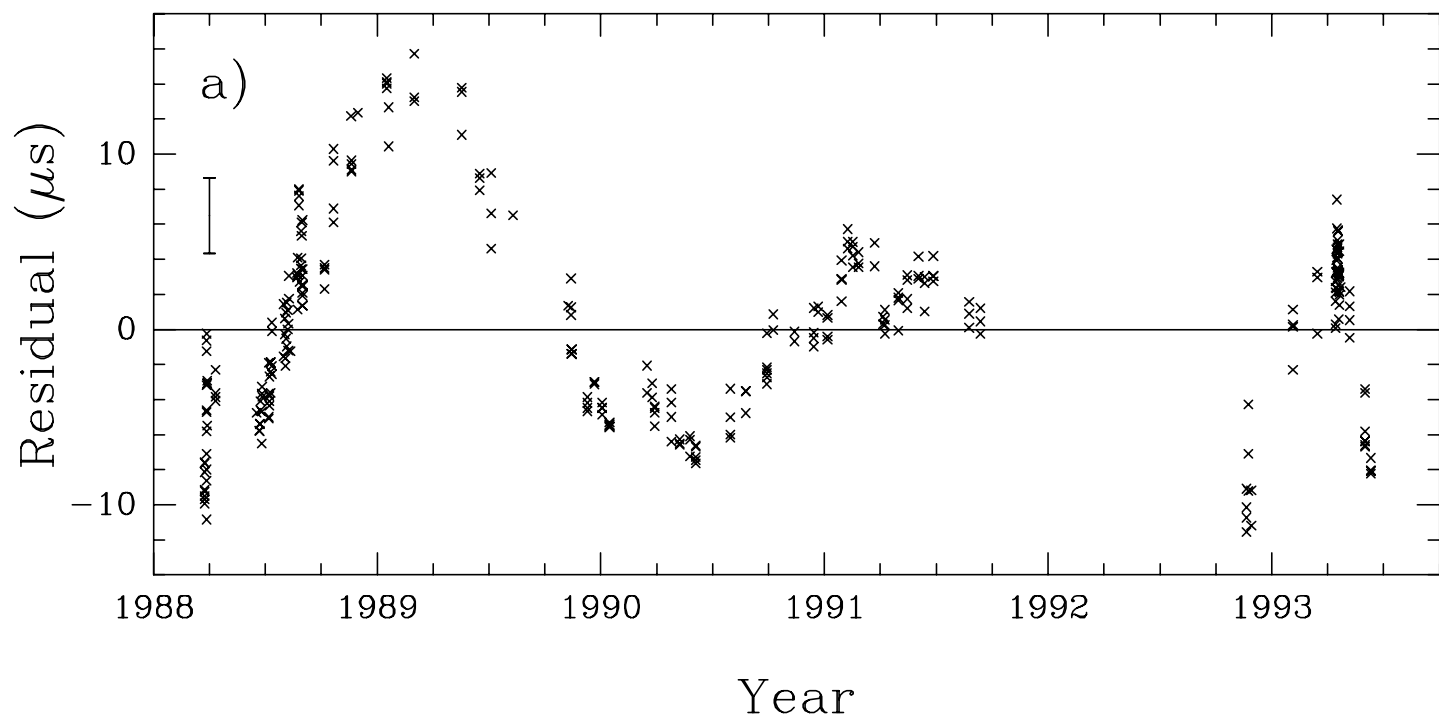
- J. R., Nice, D. J., Ryba, M. F., Stinebring, D. R., Taylor, J. H., Thorsett, S. E. & Weisberg J. M. 1990, *ApJ*, 351, 642
- Fruchter, A. S. & Goss W. M. 1992, *ApJ*, 384, L47
- Fruchter, A. S., Stinebring, D. R. & Taylor J. H. 1988, *Nature*, 333, 237
- Hall D. S. 1989, *Space Sci. Rev.*, 50, 219
- Kaspi, V. M., Taylor, J. H. & Ryba M. 1994, *ApJ*, in press
- Lyne, A. G., Biggs, J. D., Harrison, P. A. & Bailes M. 1993, *Nature*, 361, 47
- Lyne, A. G., Manchester, R. N., D'Amico, N., Staveley-Smith, L., Johnston, S., Lim, J., Fruchter, A. S., Goss, W. M. & Frail D. 1990, *Nature*, 347, 650
- McCormick, P. J., Frank, J., King, A. R. & Rajasekhar A. 1994, *ApJ*, submitted
- Nice, D. J. & Thorsett S. E. 1992, *ApJ*, 397, 249
- Nice, D. J., Thorsett, S. E., Taylor, J. H. & Fruchter A. S. 1990, *ApJ*, 361, L61
- Pasquini, L. & Lindgren H. 1993, *A&A*, submitted
- Podsiadlowski P. 1991, *Nature*, 350, 136
- Ruderman, M., Shaham, J. & Tavani M. 1989, *ApJ*, 336, 507
- Ryba, M. F. & Taylor J. H. 1991, *ApJ*, 380, 557
- Simon T. 1990, *ApJ*, 359, L51
- Söderhjelm S. 1980, *A&A*, 89, 100
- Standish E. M. 1982, *A&A*, 114, 297
- Stevens, I. R., Rees, M. J. & Podsiadlowski P. 1992, *MNRAS*, 254, 19P
- Stinebring, D. R., Kaspi, V. M., Nice, D. J., Ryba, M. F., Taylor, J. H., Thorsett, S. E. & Hankins T. H. 1992, *Rev. Sci. Instrum.*, 63, 3551
- Tavani, M. & Brookshaw L. 1992, *Nature*, 356, 320
- Taylor, J. H. & Weisberg J. M. 1989, *ApJ*, 345, 434
- Warner B. 1988, *Nature*, 336, 129
- Wijers, R. A. M. J. & Paczyński B. 1993, *ApJ*, 415, L115

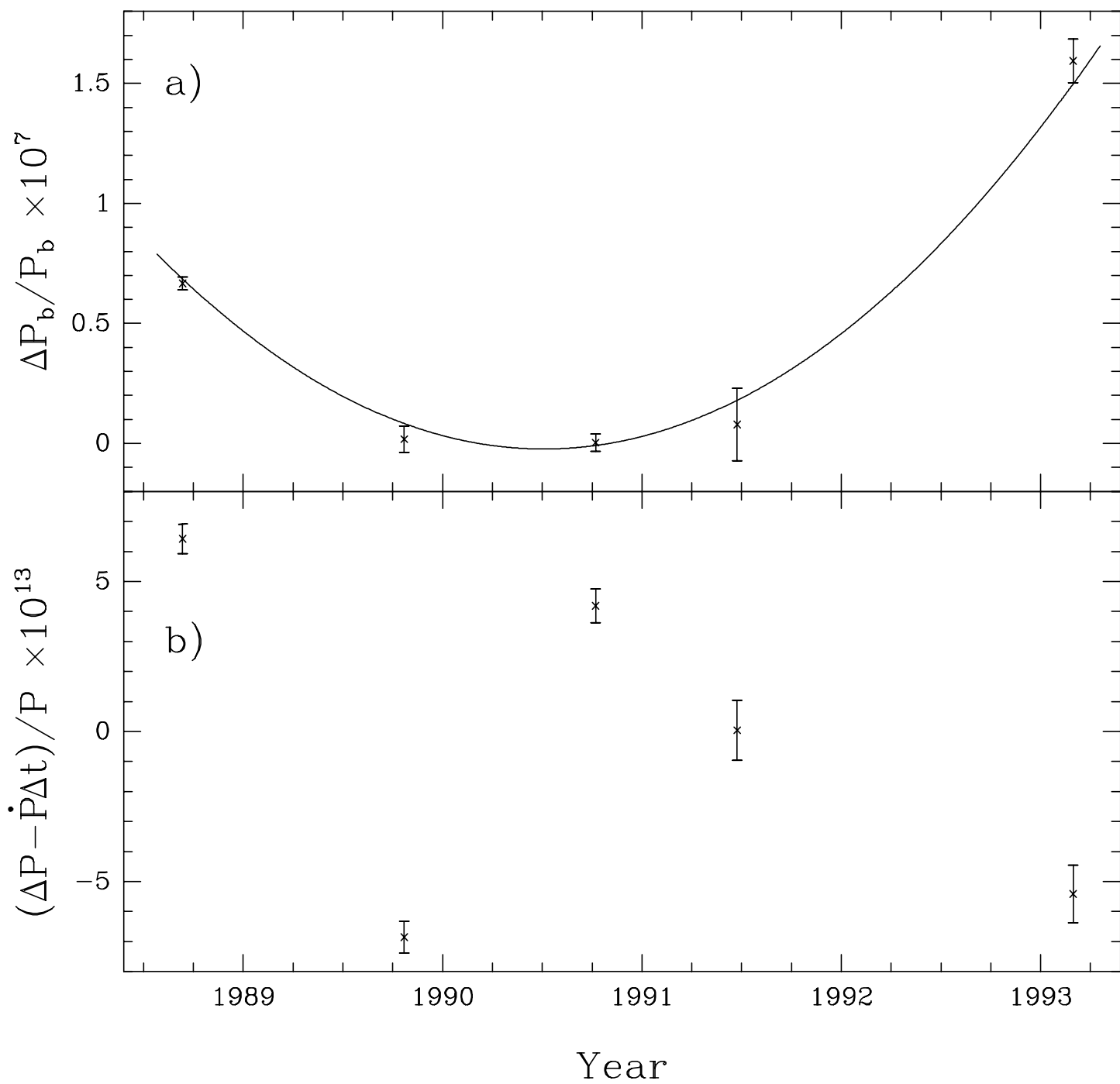
Figure Captions

Figure 1: Post-fit residuals of PSR B1957+20 plotted versus date and orbital phase. The typical uncertainty in the pulse arrival times, a few microseconds, is shown near the upper left in a).

Figure 2: a) Fractional orbital period changes in the PSR B1957+20 system versus date. The overall variation in P_b spans about 5 ms. The solid line curve corresponds to the values of P_b and its derivatives listed in Table 1. b) Fractional pulse period changes versus date. A correction has been made for the global spin-down rate given by \dot{P} in Table 1. Error bars reflect only the statistical uncertainties from the individual fits and do not include the possible effects of the long-term timing noise.

Figure 3: Orbital phase shifts (observed minus computed) in the PSR B1957+20 system. Note that the sign convention employed here is the opposite of that in the orbital phase shift plot of RT91, Figure 3. The solid line is derived from Equation (1) and the orbital information given in Table 1.





Orbital cycles

